

Mixed and mixing surface layers:  
Some observations and elements of scaling

**Louis Prieur**

L. O. V.

Prieur @obs-vlfr.fr

## Recall

Turbulence is generated / sustained by

**Driving forces:** Wind effects, shear stress  $\tau$ ,  $u^*_w = (\tau/\rho_w)^{1/2}$ ;  $\tau = C_d \cdot \rho_a \cdot U_{10} \cdot |U_{10}|$   
Buoyancy flux (losses of buoyancy, ocean cooling)  $J_b$  or  $B_o$  ( $m^2 \cdot s^{-3}$ )

**Surface effects** (waves, langmuir cells)

**Internal waves, submesoscale and mesoscale instabilities**

## Concern

Ocean depth mixed layer  $H_{md}$ , few meters to 2000 m;  $\delta\rho < 0.01 \text{ kg/m}^3$  one among many criteria

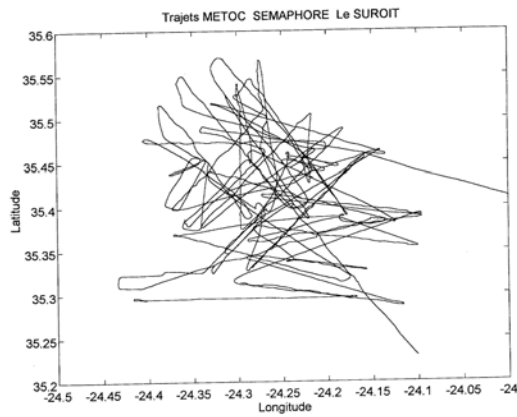
Special attention when  $H_{md} > Z_e$

Mixing layer depth (active) against Mixed layer depth ?

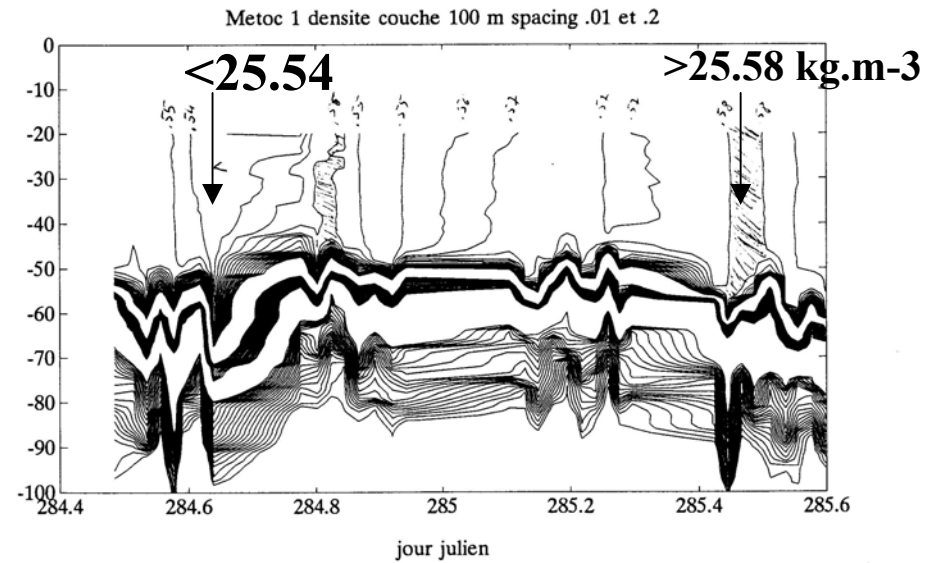
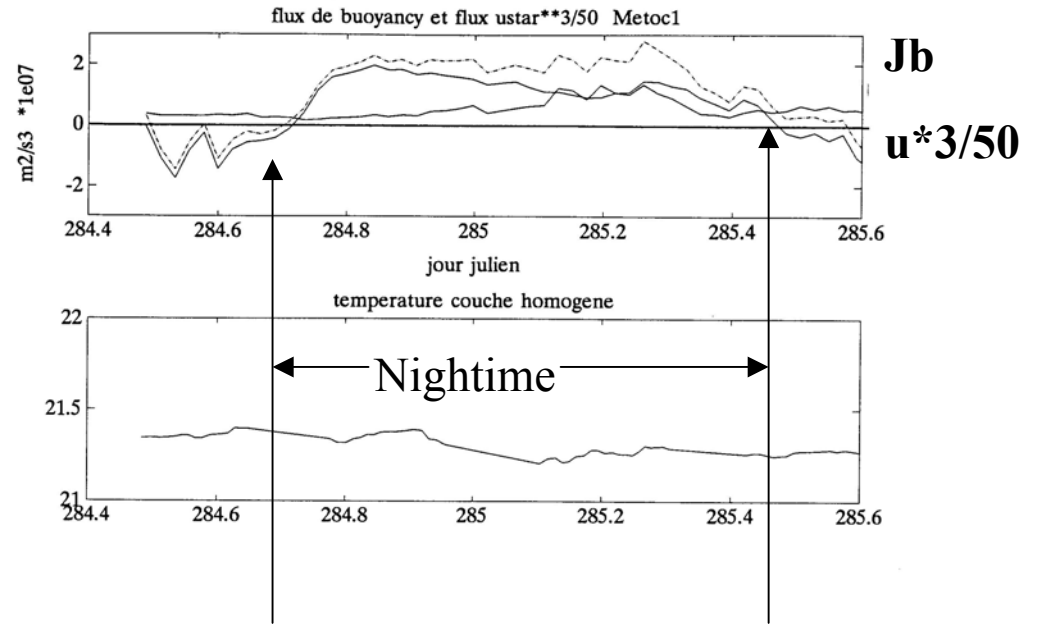
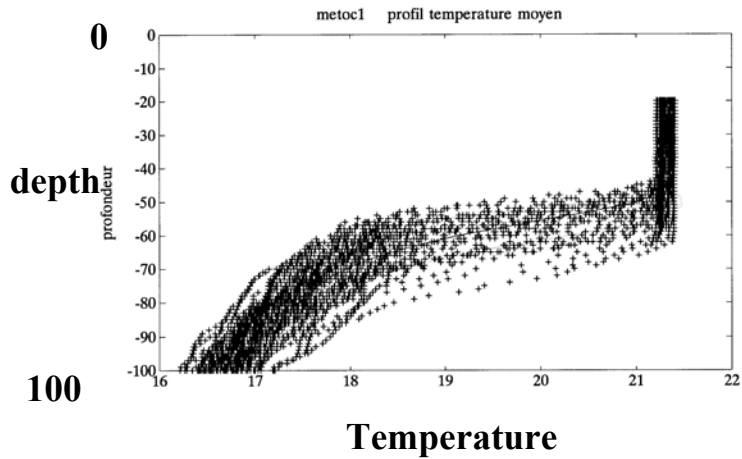
## Questions

**Cycling time of water parcel?  $T_{conv} = H/w$ ;  $w?$   $u^*?$**

# SEMAPHORE



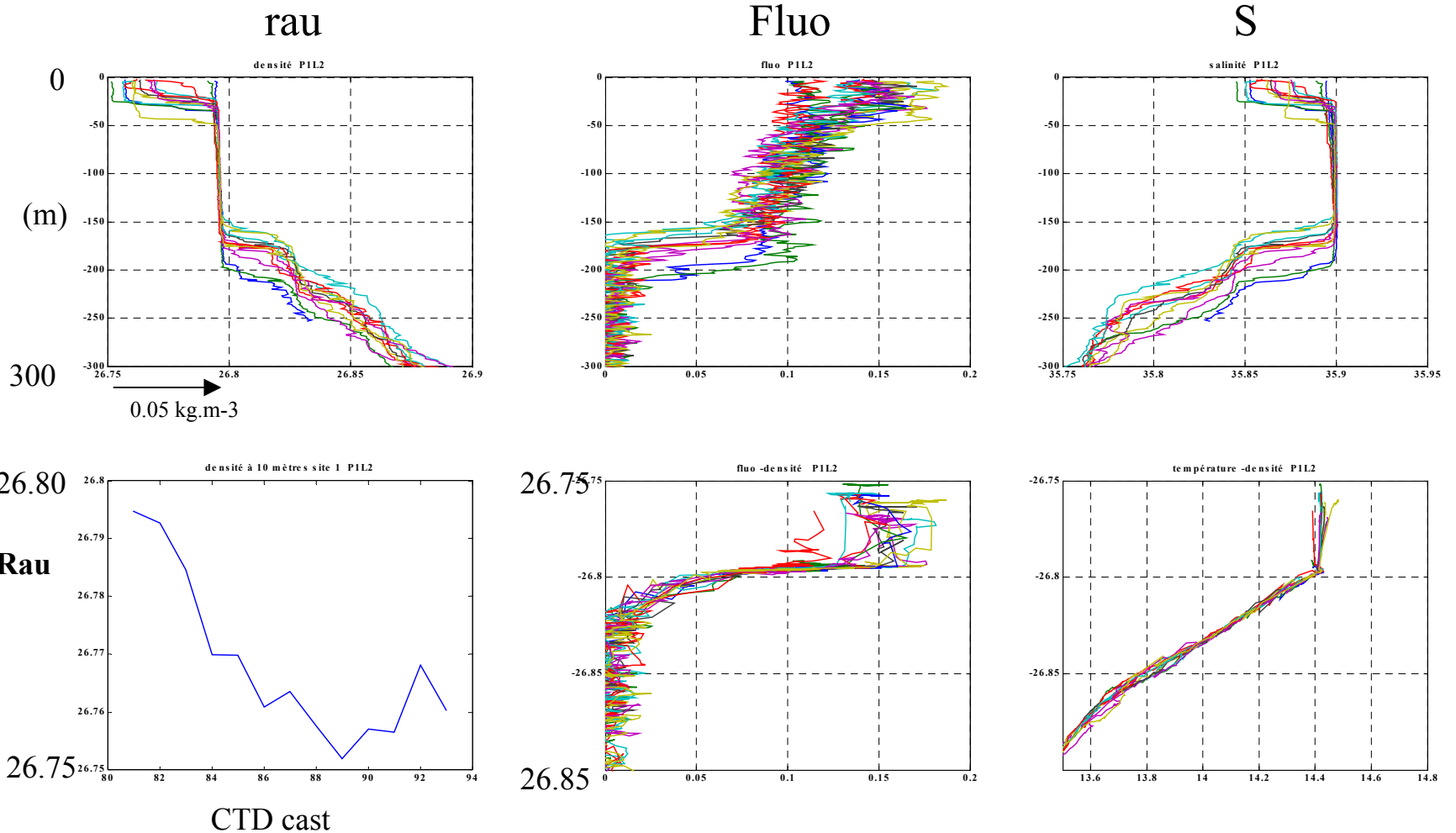
20 km \* 20 km TOWYO

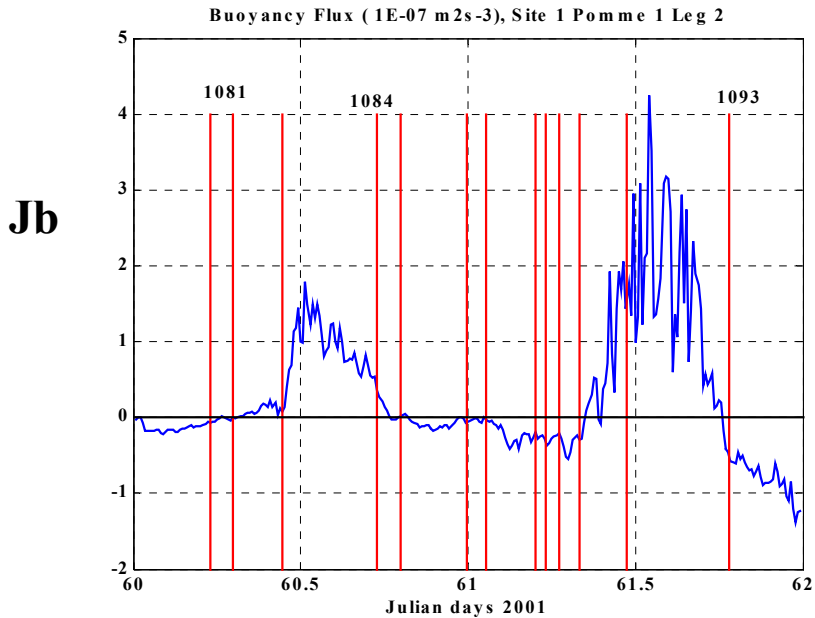


Deltarau vert. << delta rau horiz.

# NE Atlantic, 40°N, 18°W, 1st-2nd March 2001, 13 casts 2 days

## Site 1 Pomme 1 Leg 2





**Start (1081 cast): 180 m mixed layer, Fluo Homogeneous**

**Depth of euphotic layer: ca 60-70 m**

**Rains after 1082 ? + Low Jb losses  $\longrightarrow$  Stratification**

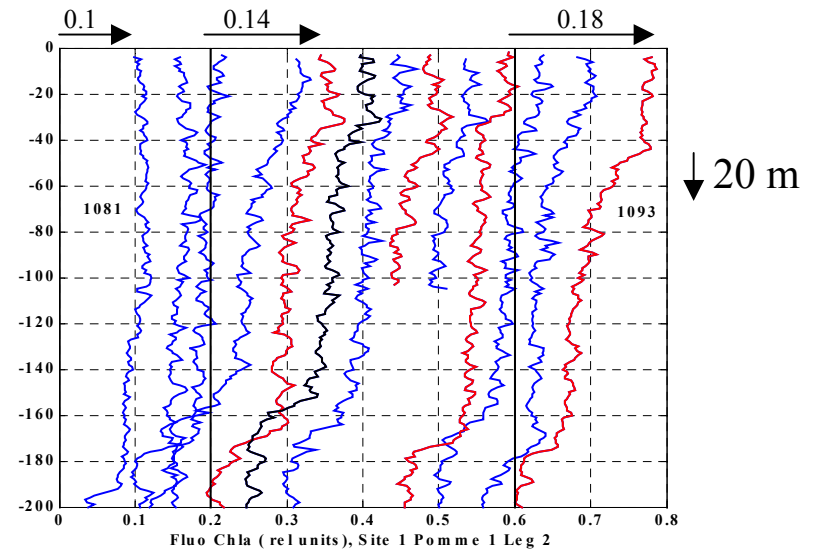
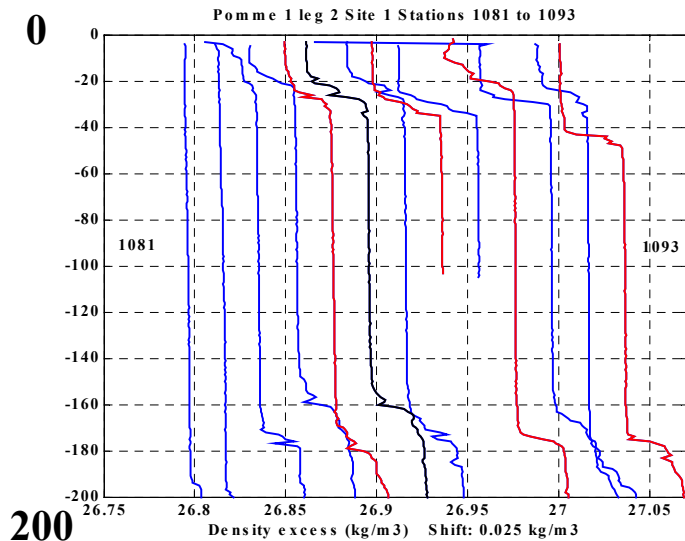
**Turbulence (convection) limited to 40 m upper layer**

**Doubling Biomass for 2 days**

**Biomass did not change in 40-180 m layer**

**Production was limited by turbulence for 1081-1082 casts**

**C – depth profiles lagged 0.05**



**Rau – depth profiles lagged 0.02 kg/m<sup>3</sup>**

## Increasing C for 2 days in the 50 m upper layer (mixing layer)

$$\mu \cdot C \cdot H_{mg} > K_z \cdot \delta C / \delta z \Big|_{-H_{mg}}$$

$$K_z < (\mu \cdot H_{mg} \cdot \delta z) \cdot C / \delta C$$

$$0.5 \cdot 50 \cdot 20 \cdot 1$$

$$K_z < 500 \text{ m}^2\text{d}^{-1}$$

But same kind of calculation inside the mixing layer  $H_{mg}$

No gradient in C, same  $\mu$

$$C / \delta C > 10 \text{ on } 25 \text{ m (} H_{mg} \text{ and } \delta z \text{)}$$

$$K_{mg} > 0.5 \cdot 25 \cdot 25 \cdot 10$$

$$K_{mg} > 3125 \text{ m}^2\text{d}^{-1}$$

**However K formulation non relevant in mixing layer  
(Ex  $H_{mg} > 50 \text{ m}$ ;  $K_{mg} > 12500 \text{ m}^2\text{.d}^{-1}$ ; not realistic,  
upper limit:  $2500 \text{ m}^2\text{.d}^{-1}$  ; towards 3D )**

**C – profiles are very sensitive to  $H_{mg}$  and  $K_{mg}$  or  $W$**

**What about time fluctuation ?**

**$J_b$  time scale,  $u^*$  time scale?**

**$J_b$  same dimension as  $u^*3/H_{md}$  and  $\epsilon$   $m^2s^{-3}$**

**Epsilon :coefficient of eddy kinetic energy dissipation**

**involved in mixing length estimation**

**also in size estimation of the largest eddy**

**$L_o = (\epsilon^{1/2} \cdot N^{-3/2})$  Ozmidov length;  $N^2 = -g/\rho \, d\rho/dz$**

◆ **Surface Buoyancy flux ; >0 if stratifying**

(m<sup>2</sup>.s<sup>-3</sup>) ou (w.kg<sup>-1</sup>)

$$J_b \equiv -\frac{g}{\rho_0 \cdot C_p} \cdot \alpha \cdot Q_{net} + \beta \frac{g}{\rho_0 L_v} \cdot S \cdot Q_e \quad (-u^*3/Hmd)$$

**Q<sub>net</sub>**      Net surface flow of heat towards Ocean

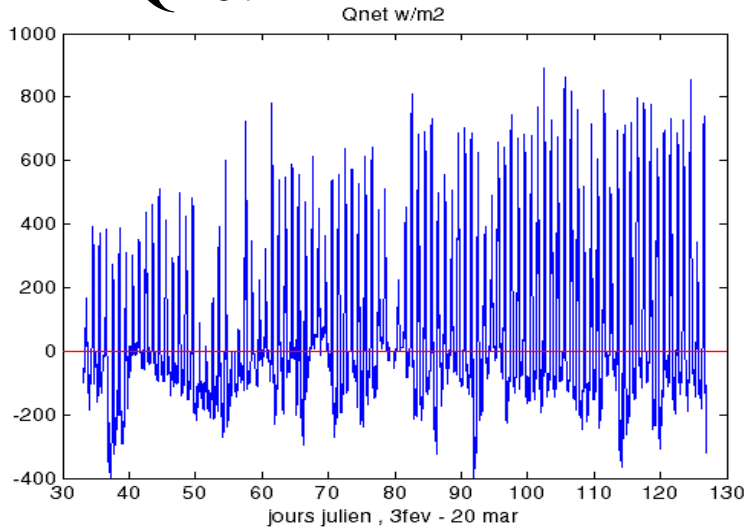
**Q<sub>e</sub>**      Heat losses by zvaporation as estimate of the amount water losses (change in S)

**α and β**      thermal and haline expansion coefficient of seawater

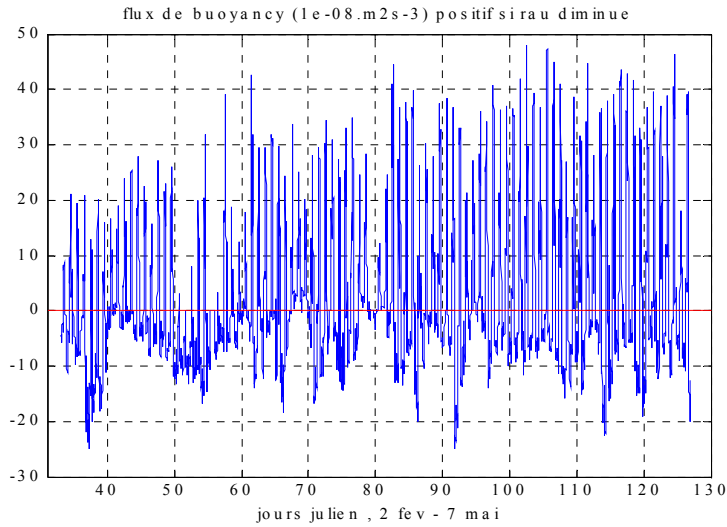
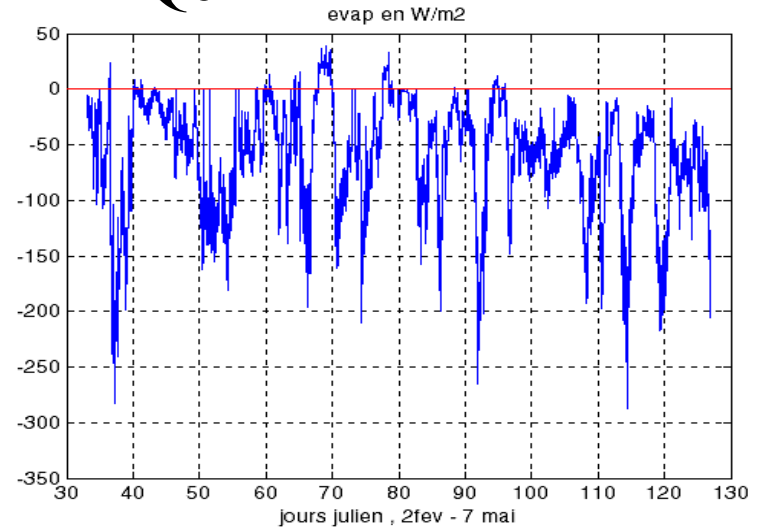
◆ **How do J<sub>b</sub>, Q<sub>e</sub>, Q<sub>net</sub> vary?**

◆ **Example from Pomme**

# Qnet



# Qe

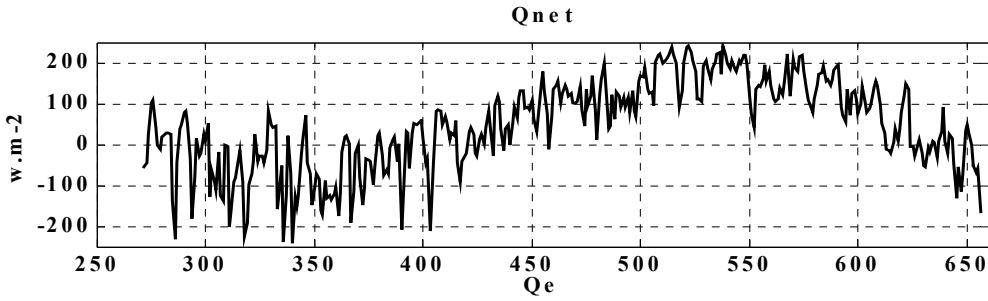


# Jb

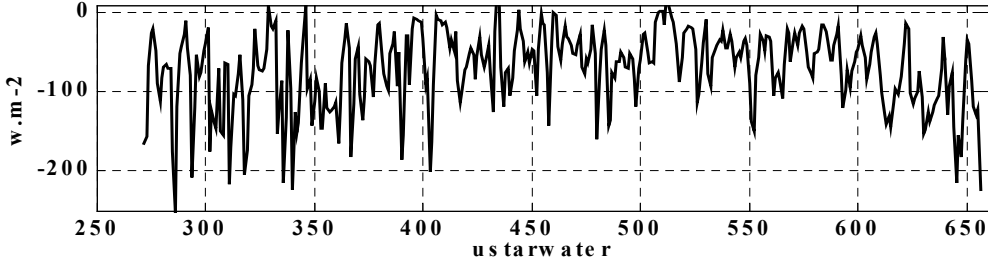
Strong diel variations  
of Jb, ca  $\sim 4e-07$  m<sup>2</sup>.s<sup>-3</sup>

← Time 100 days →

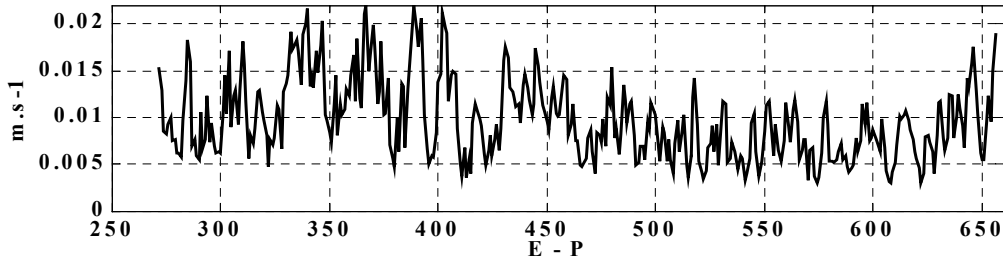
Qnet



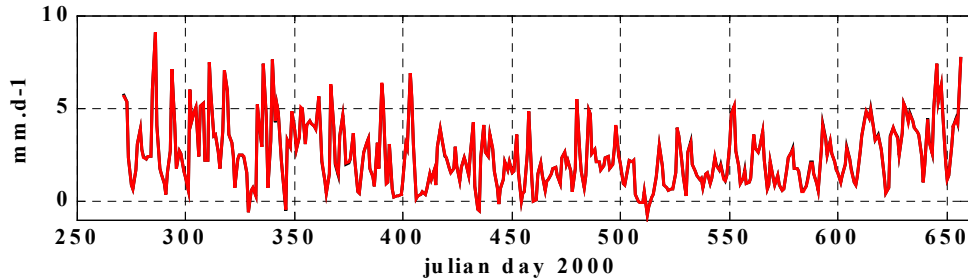
Qe



u\*<sub>w</sub>



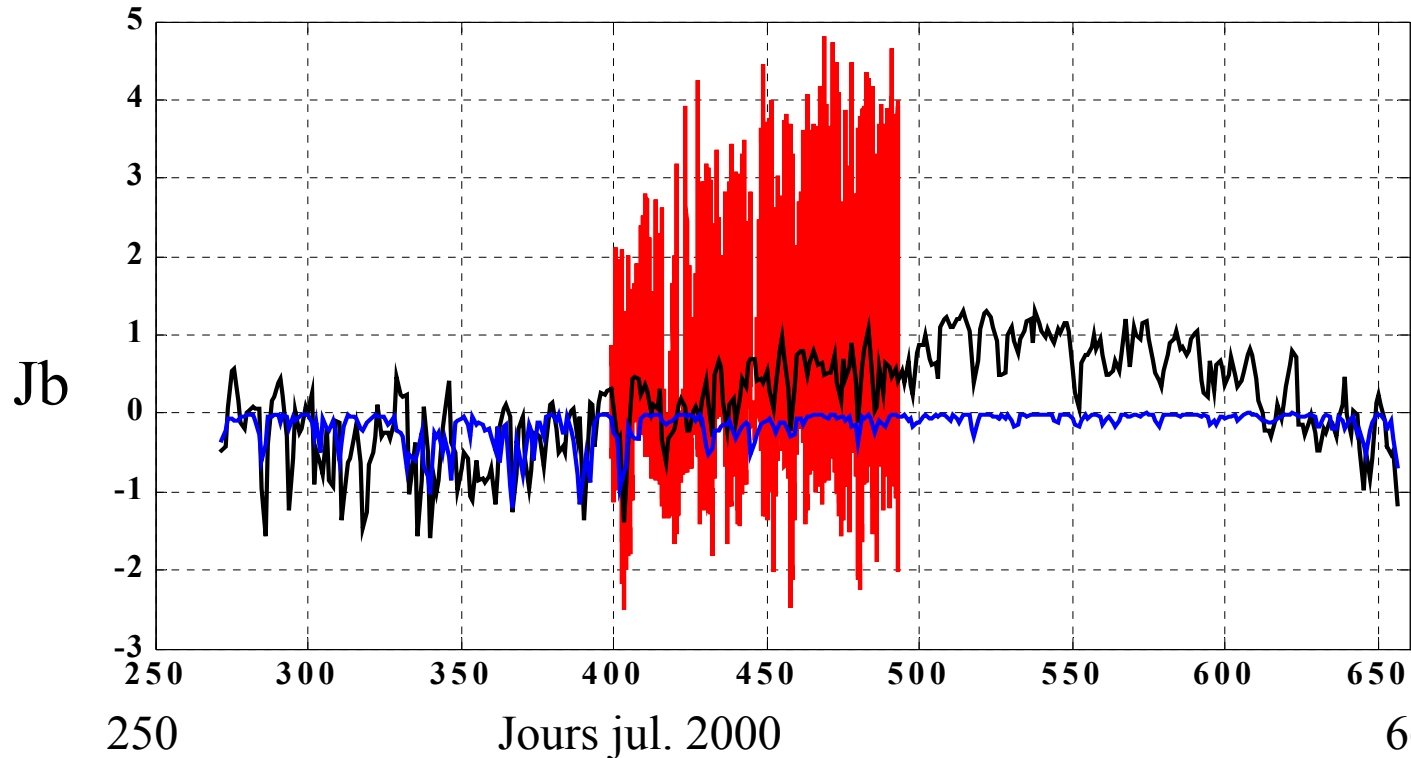
E-P



← Time 368 days →

Strong variations of  $J_b$  along a day and between successive days

$10^{-7} \text{ m}^2\text{s}^{-3}$  Pomme Buoyancy flux ( $\times 10^7 \text{ m}^2\text{s}^{-3}$ ) and  $u^*3/100$



Jb daily aver.

Jb 10 min.

$u^*3/100$

# Mixed layer, mixing layer, remnant layer

1526

K. E. Brainerd and M. C. Gregg

DSR 1995

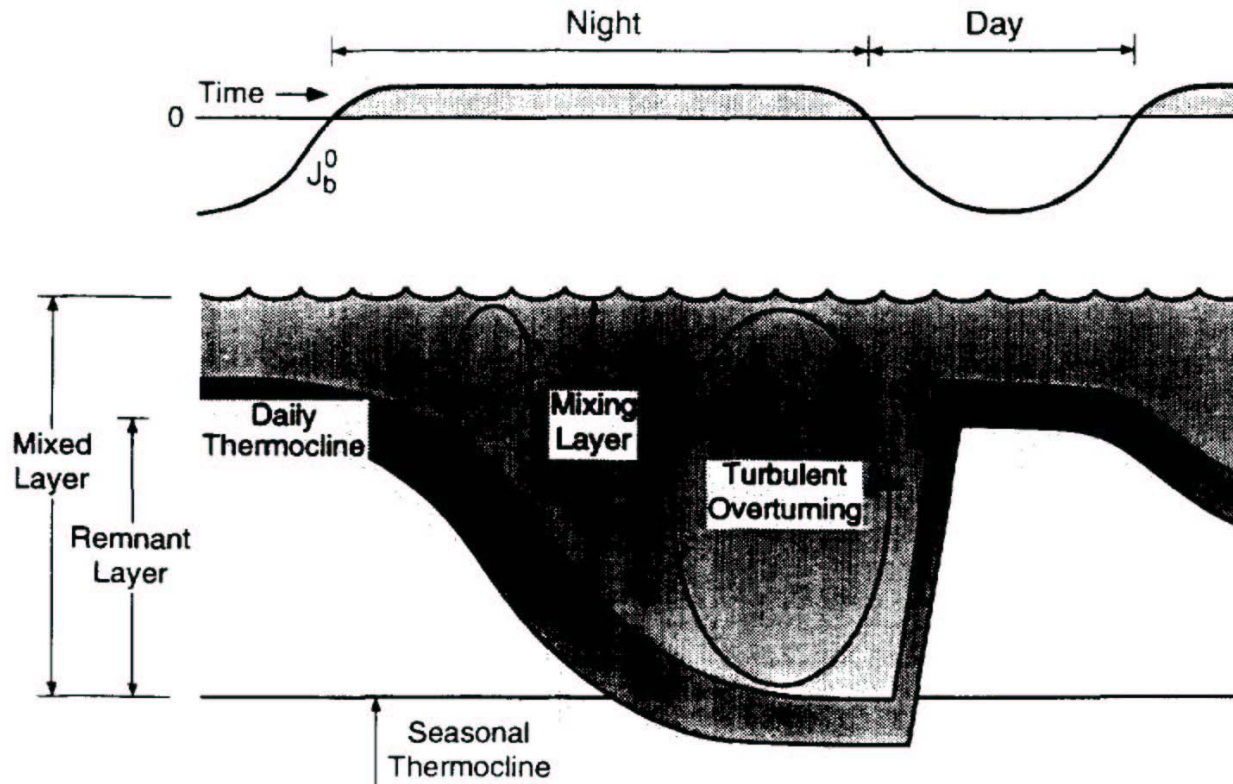


Fig. 5. Diagram showing depth zones in a typical diurnal mixed layer cycle.

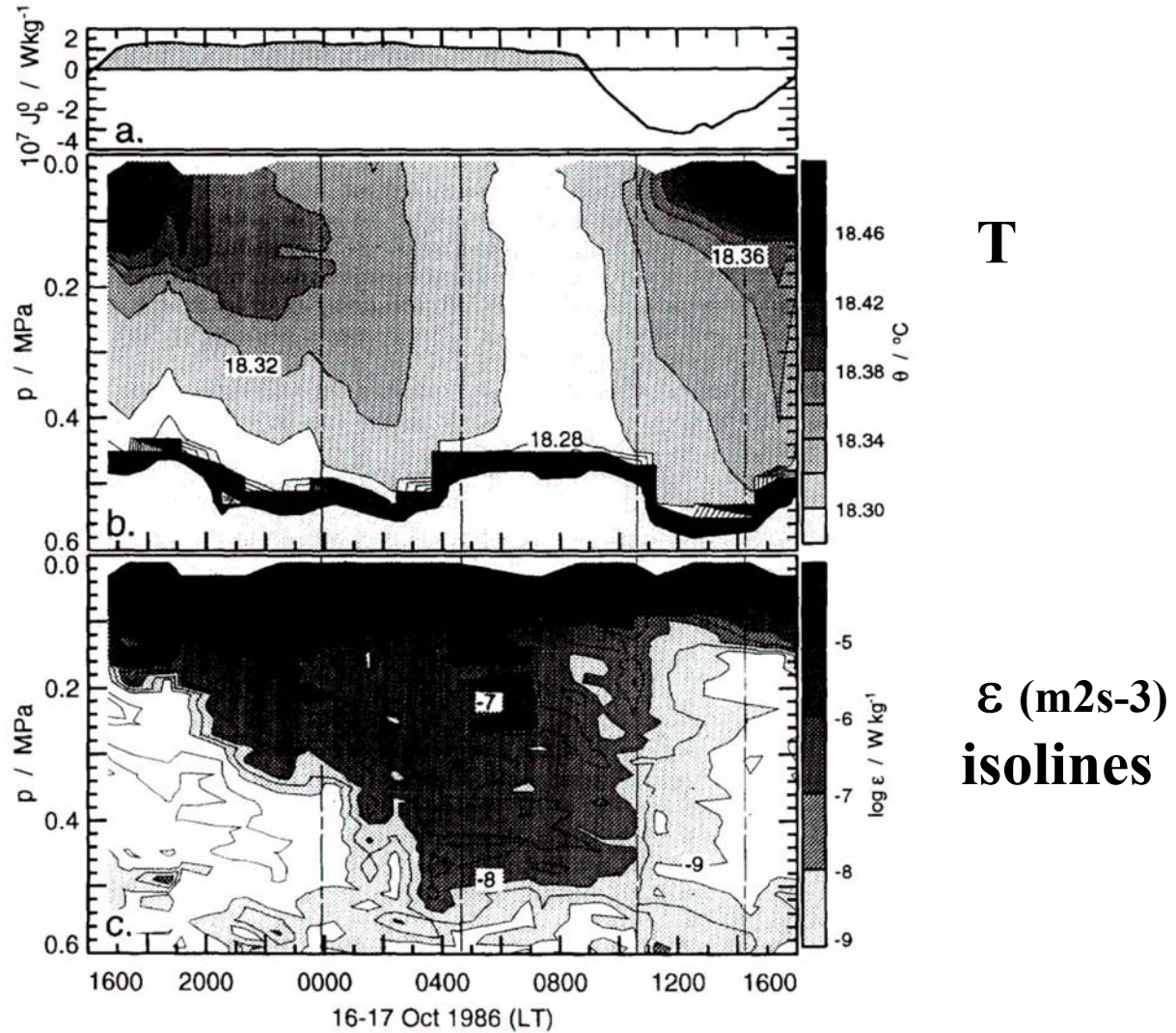


Fig. 6. A one-day cycle from PATCHEX. The vertical dashed lines mark the times of profiles shown in Fig. 7. Panel a. Surface buoyancy flux  $J_b^0$ . Panel b. Contours of  $\theta$ , hour averages in 2 m vertical bins. Contour interval  $0.02^\circ\text{C}$ . Heavy black line is the top of the seasonal thermocline. Panel c. Contours of  $\log \epsilon$ ; hour averages in 2 m vertical bins. Contour interval 0.5.

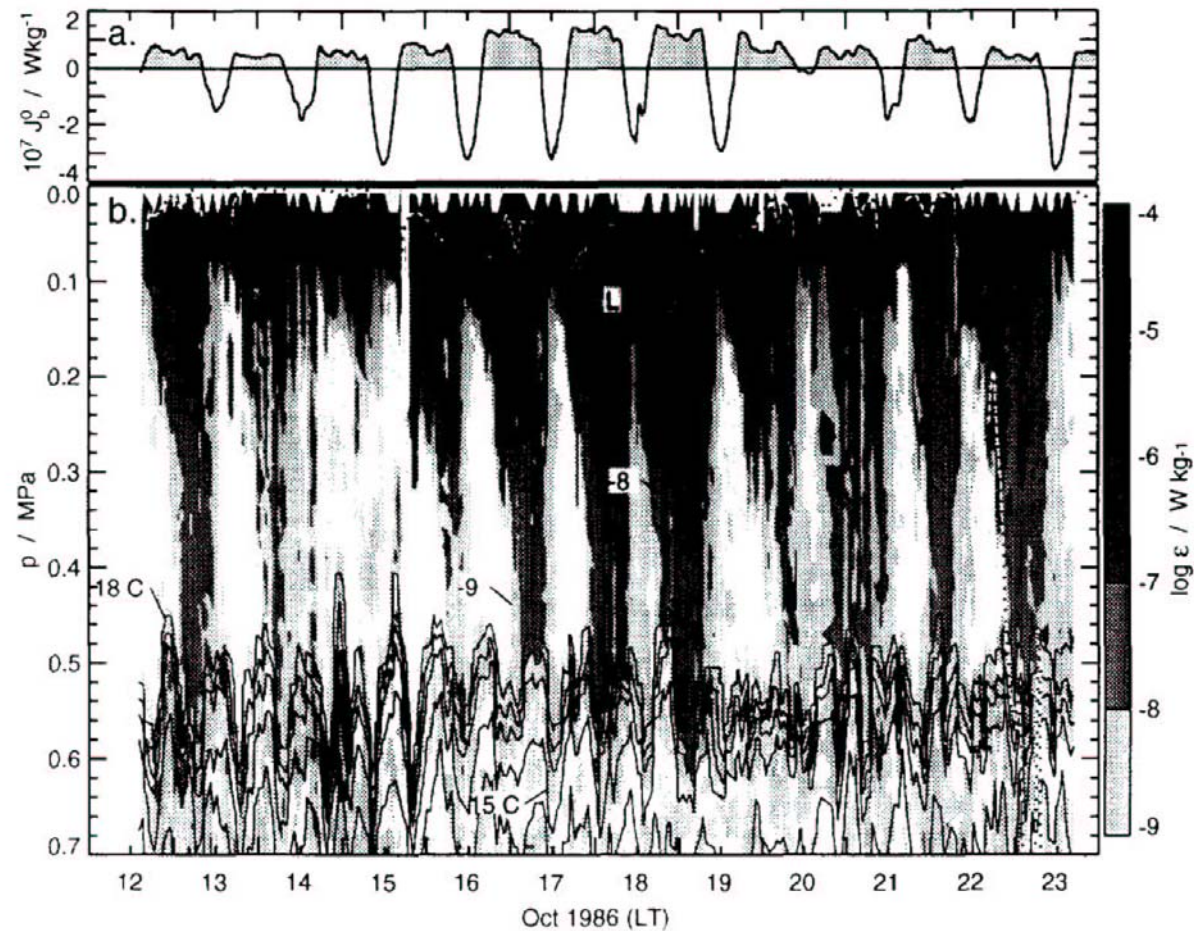


Fig. 3. Summary of turbulent dissipation rates on PATCHEX. Panel a. Surface buoyancy flux  $J_b^0$ . Shaded parts mark periods when convection is being forced (cooling). Panel b. Shaded contours are  $\log \epsilon$ ; solid lines are isotherms ( $1^\circ$  contour interval), suggesting the depth of the thermocline. Heavy dashed line is Monin-Obukhov length ( $L$ ), plotted by taking 1 MPa to be equivalent to 100 m.

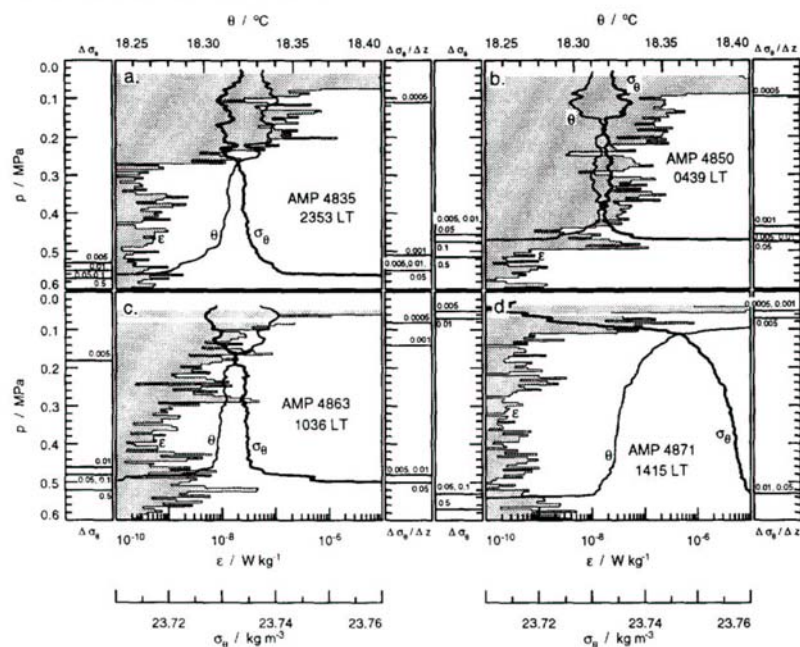


Fig. 7. Profiles of  $\epsilon$ ,  $\theta$  and  $\sigma_\theta$  taken at four stages of the daily cycle shown in Fig. 6. The shading is  $\epsilon$ , estimated in 0.5 m bins;  $\theta$  and  $\sigma_\theta$  have been processed with a 0.8 m triangular filter. Horizontal lines in the side panels mark values returned by the mixed layer depth criteria; density difference criteria on the left hand panels, density gradient criteria on the right. Panel a. Drop 4835; 2353 LT, 16 October 1986, during convective deepening phase. Panel b. Drop 4850; 0439 LT, 17 October 1986, during convective equilibrium phase. Panel c. Drop 4863; 1036 LT, 17 October 1986; start of growth of diurnal thermocline. Panel d. Drop 4871; 1415 LT, 17 October 1986; diurnal thermocline has become quite strong.

series of profiles from PATCHEX. Figure 7 shows profiles taken at four times in the daily cycle shown in Fig. 6. The profile in panel a was taken during convective deepening. From  $\epsilon$ , it appears that convection was active down to about 0.26 MPa. The depth range between 0.26 and 0.28 MPa is the entrainment zone, within which  $\epsilon$  decreases rapidly, and  $\sigma_\theta$  transitions between the nearly unstratified mixing layer above and the stratified remnant layer below. The density and temperature profiles show many overturns within the mixing layer, but the mean has nearly neutral stability; within the entrainment zone  $\sigma_\theta$  shows a small increase of about  $0.003 \text{ kg m}^{-3}$ . This increase is of the same magnitude as the overturns seen above it, and none of the density step depth criteria are able to detect it. A density gradient of  $(\Delta\sigma_\theta)_c = 0.005 \text{ kg m}^{-4}$  triggers on an overturn within the mixing layer; larger values of  $(\Delta\sigma_\theta)_c$  find the seasonal thermocline. Panel b of Fig. 7 shows a profile taken during the convective equilibrium phase, when convection extends down to the

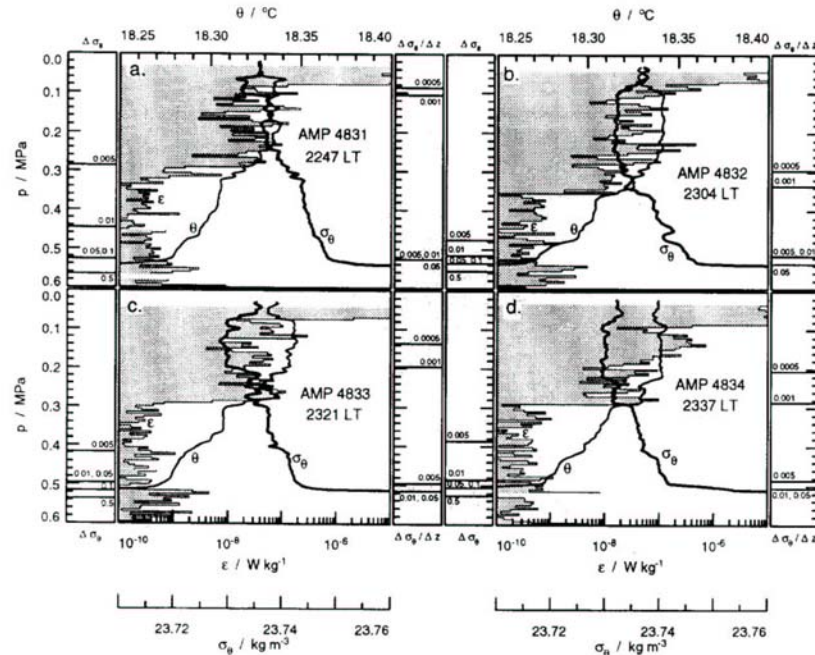


Fig. 9. Profiles of  $\epsilon$ ,  $\theta$  and  $\sigma_\theta$  from four consecutive drops during convective deepening on 16 October, from PATCHEX. The shaded line is  $\epsilon$ , estimated in 0.5 m bins;  $\theta$  and  $\sigma_\theta$  have been processed with a 0.8 m triangular filter. Horizontal lines in the side panels mark values returned by the mixed layer depth criteria; density difference criteria on the left hand panels, density gradient criteria on the right. Panel a. Drop 4831; 2247 LT. Panel b. Drop 4832; 2304 LT. Panel c. Drop 4833; 2321 LT. Panel d. Drop 4834; 2337 LT.

distinction between the mixing and mixed layers. Judging the mixing layer depth from  $\epsilon$ , it can be seen that the mixing depth is highly variable from one night to the next, reaching maximum depths between 0.2 and 0.7 MPa, and only occasionally extends down to the seasonal thermocline, the top of which is near 0.7 MPa; the depth of the top of the seasonal thermocline is set only by occasional deep mixed layer events. The strong day to day variability in mixing layer depth appears to be related to the strong remnant layer stratification (Fig. 11) that usually prevents convection from penetrating to the seasonal thermocline at night.

In order to show the overall performance of the two types of criteria, Fig. 12 compares the range of mixed layer depth definitions with the observed overturning for one typical day. As in the PATCHEX case (Fig. 8), the density difference criteria  $(\Delta\sigma_\theta)_c = 0.005$  and  $0.01$  follow the daily mixing cycle reasonably well, while none of the other criteria do.

In this cruise the surface forcing was dominated by squalls, which frequently included very heavy rainfall. This emphasizes the possible importance of salinity to mixed layers;

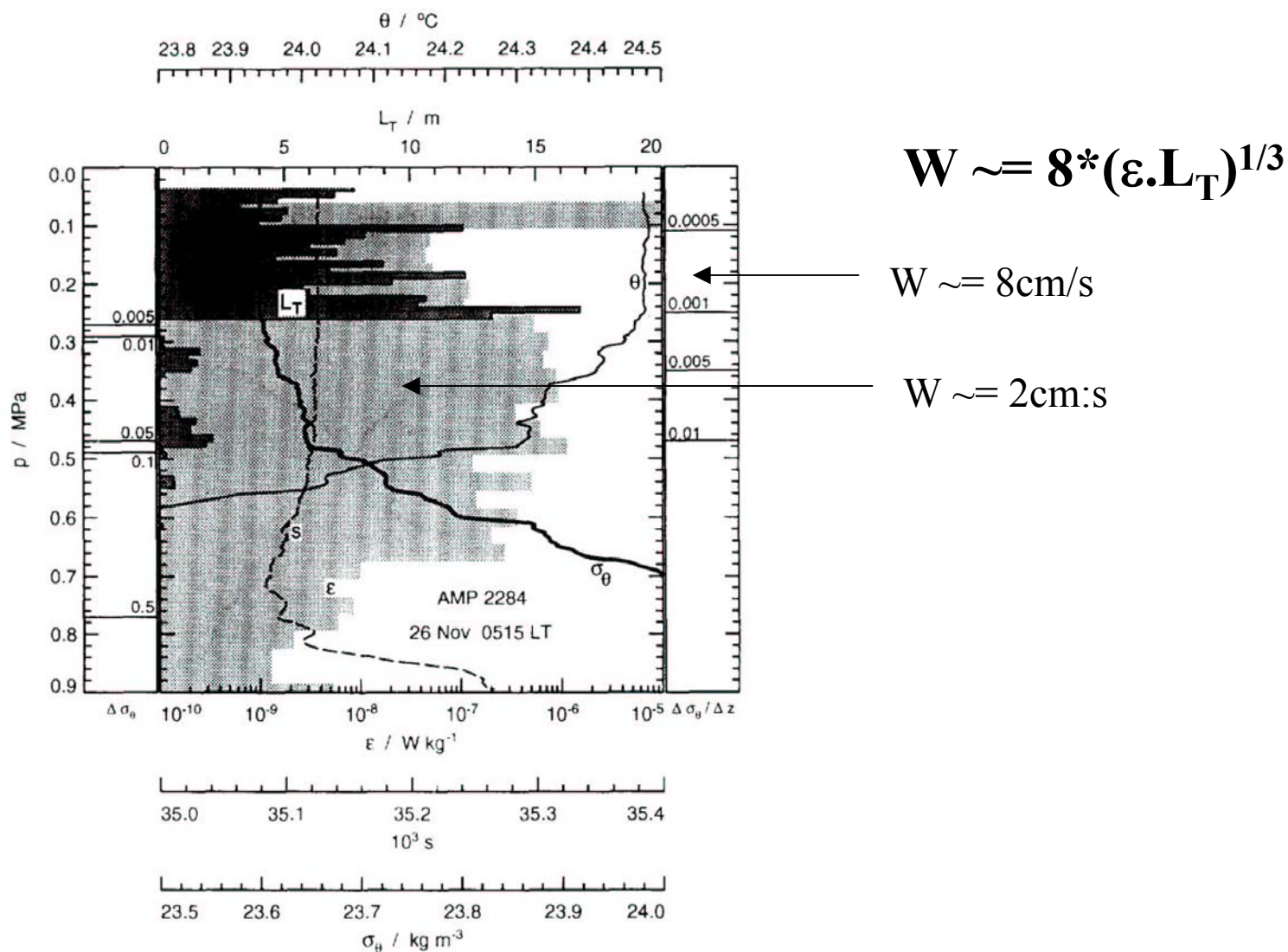


Fig. 15. Profile from the Tropic Heat Cruise:  $\theta$  (thin solid line),  $\sigma_\theta$  (heavy solid line), salinity (dashed line), and  $\epsilon$  (shaded).  $\theta$  and  $\sigma_\theta$  are well-mixed down to 0.2 MPa, although strong turbulence extends past 0.8 MPa.

**Brainerd and Gregg , DSR Sept. 1995:**

**mixed layer rather shallow (60 to 100 meters)**

**observations of  $L_T$ , epsilon**

**$W_{mg} \approx 2$  to 8 cm/s;  $T_{conv} \text{ ca } 30$  min**

**Close to estimation by Denman L&O 1983 from scaling arguments**

**Now observation by Lagrangian 3D floats,**

**Deep mixed layer**

**Steffen and d'Asaro JPO Feb 2002**

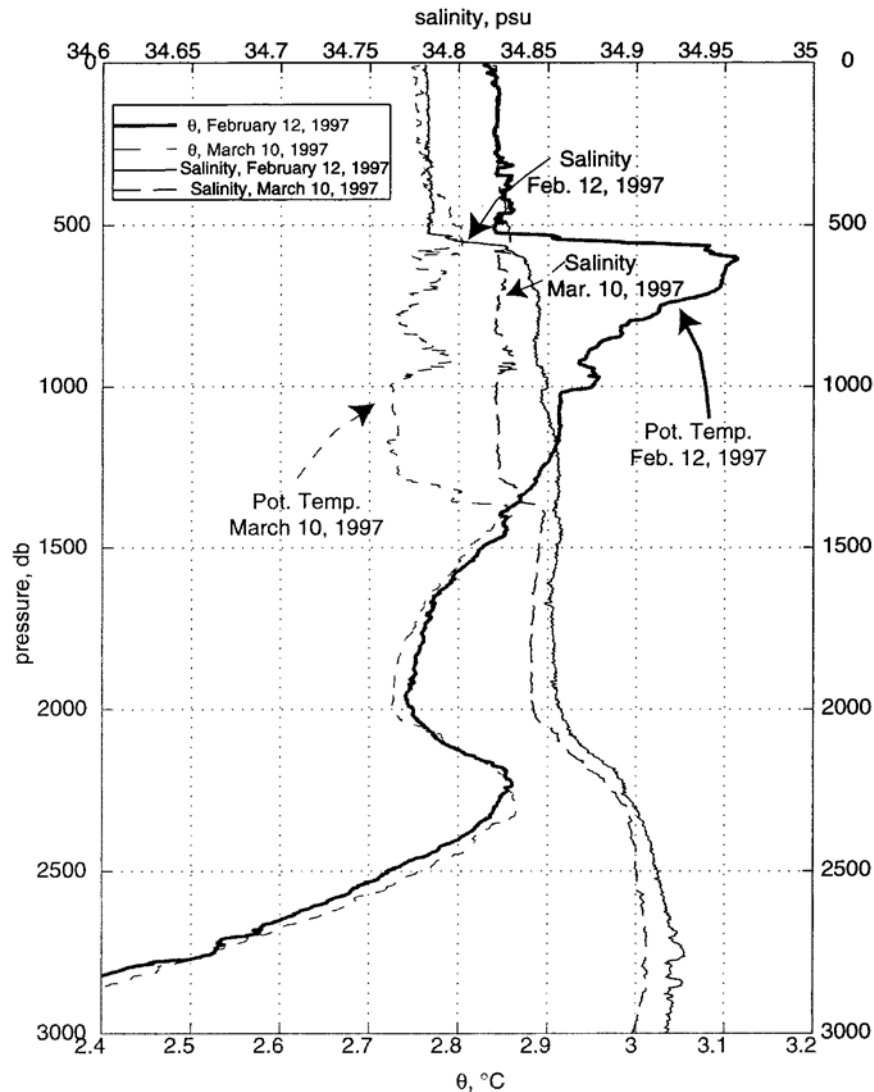


FIG. 1. Two CTD casts from R/V *Knorr* Cruise 147 (data courtesy of R. Pickart): from station 9 (solid lines), 12 Feb 1997 (at DLF deployment time and location), and station 119 (dashed lines), 10 Mar 1997 (at DLF deployment location and mission end time). The characteristic stratification for this region is visible in both stations: the relatively cold, fresh mixed layer overlies warmer, saltier water. During the month between these two casts, the mixed layer deepened from about 530 to 1320 db. During this deepening the salt has been mixed, but overall salt content has remained essentially constant in the upper 1300 db.

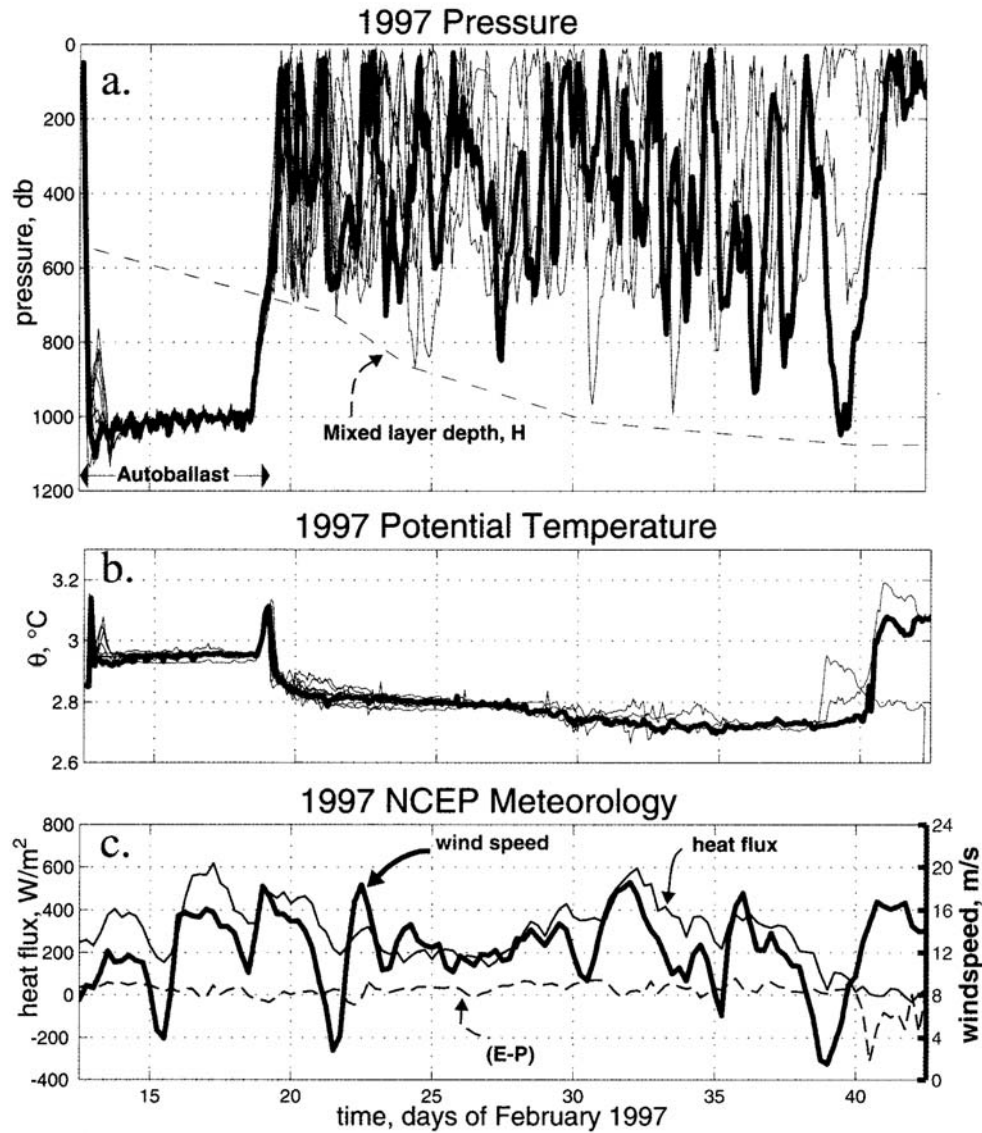


FIG. 5. 1997 records: (a) Pressure. All 13 floats shown solid, float 12 shown bold. Although 13 floats begin the record, only 3 remain at the end due to gradual failures throughout. Dashed curve is a rough representation of the mixed layer depth. (b) Temperature. (c) NCEP meteorological data. Dashed line indicates the equivalent heat flux of evaporation minus precipitation—the amount of heat flux necessary to produce the same change in buoyancy produced by the haline flux. Total heat flux (thin solid) has had a 1-day running mean applied. Wind speed (thick solid) corresponds to y axis at right.

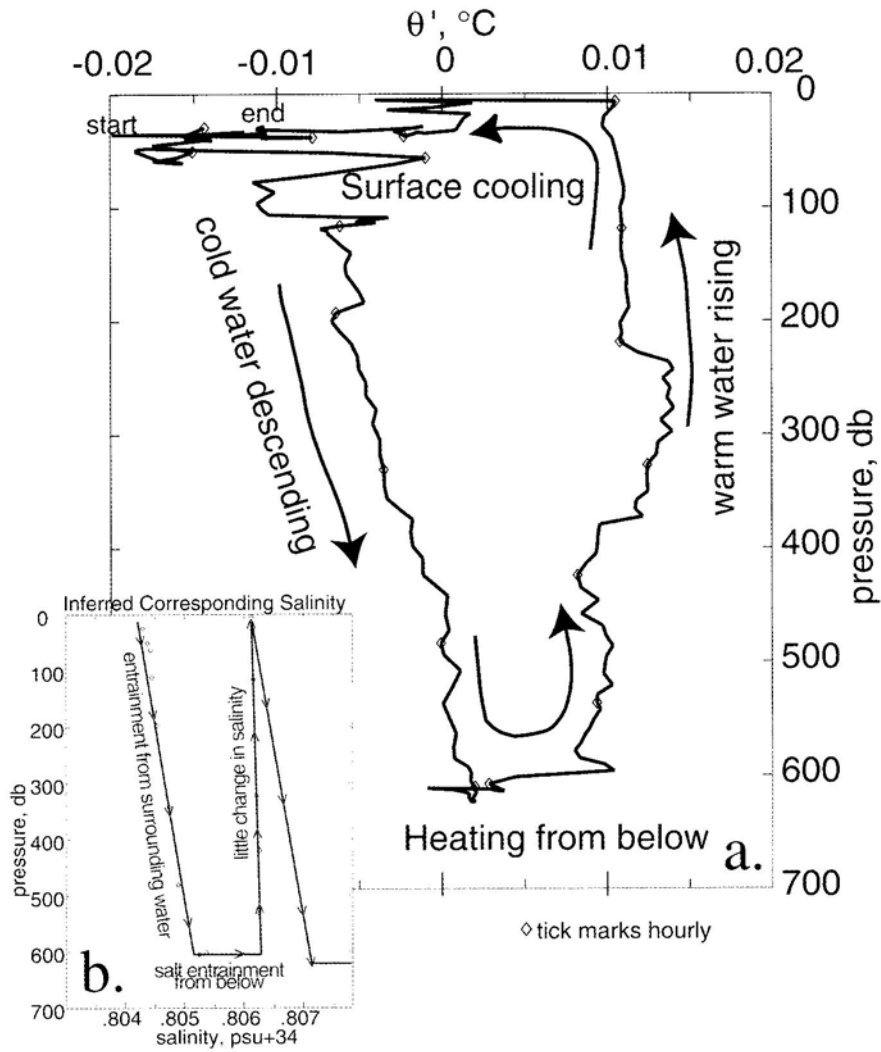


FIG. 12. (a) A trajectory in temperature, pressure space graphically illustrates the behavior of the mixed layer to be that of a vertical conveyor belt of heat. (b) The hypothetical accompanying change in salt.

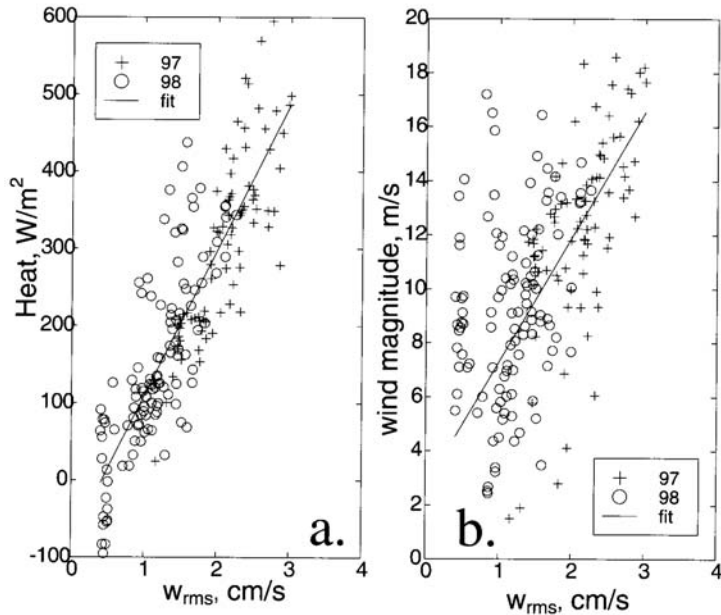


FIG. 15. Scatterplots of lagged meteorological data paired with observed rms vertical velocity; linear fits shown solid.

Fit :  $w = a * w_{nonrot} + b * w_{rot}$       $a = 0.5$  ;  
 $b = 0.05$ , 13 floats, skill (75%)

$$w_{nonrot} = (Jb * Hmd)^{1/3} \quad ;$$

$$w_{rot} = (Jb/f)^{1/2}$$

$w_{nonrot}$  predominant here

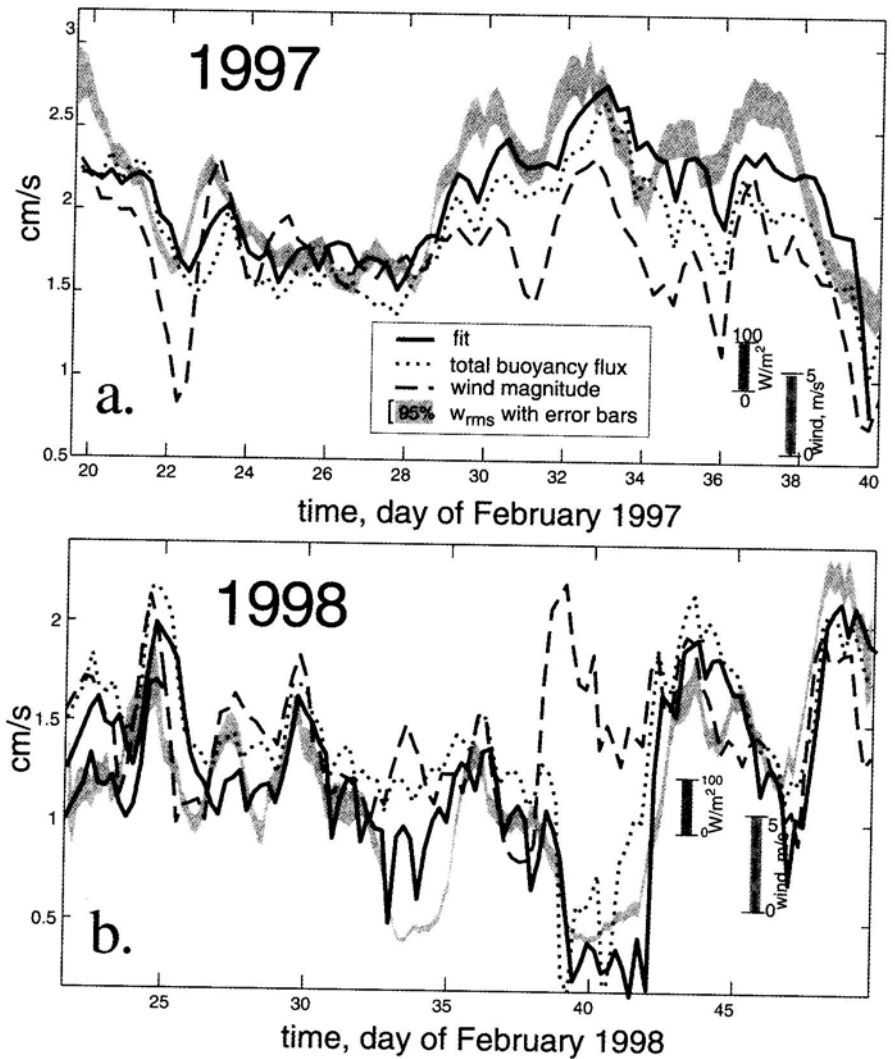
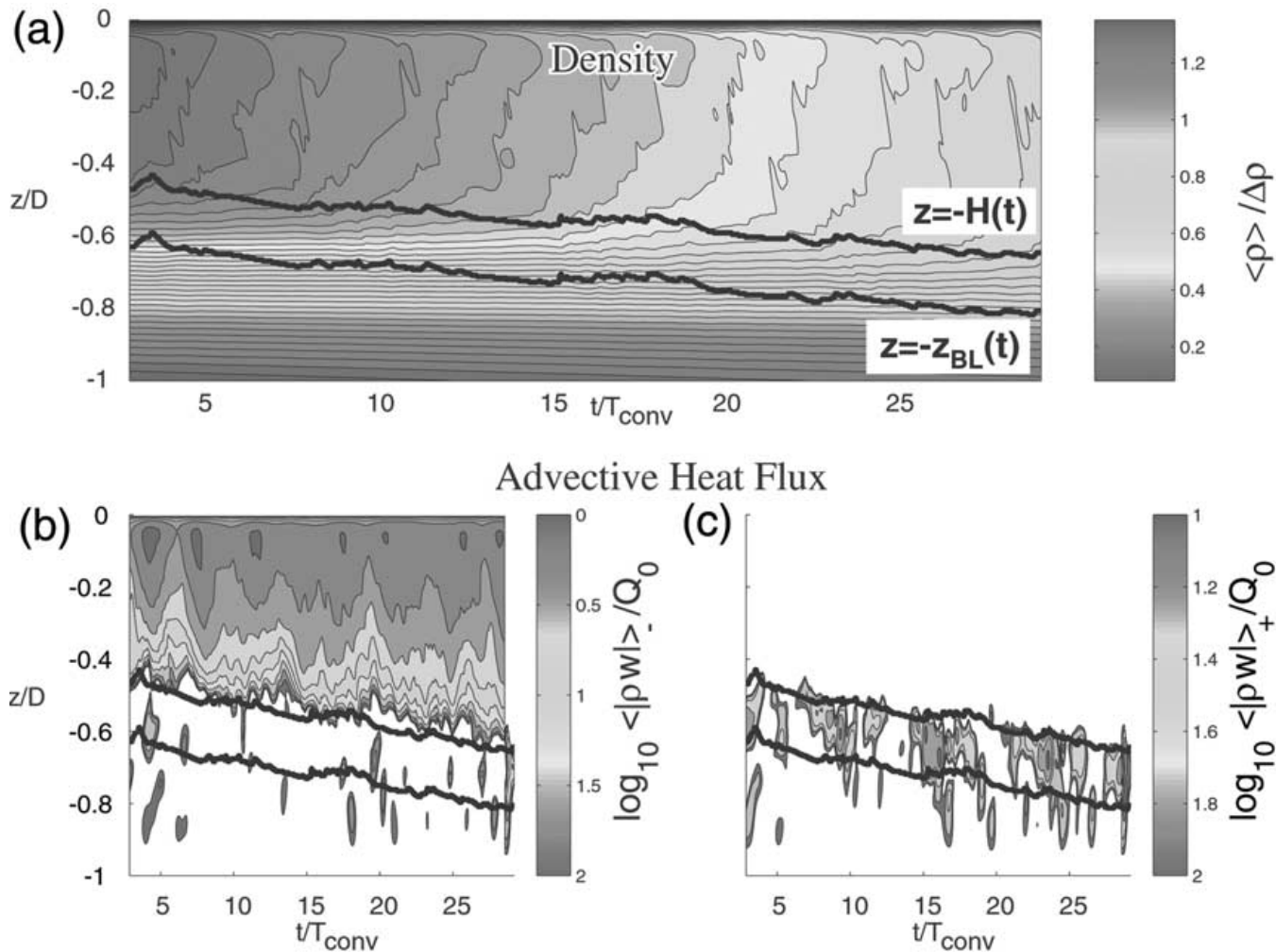
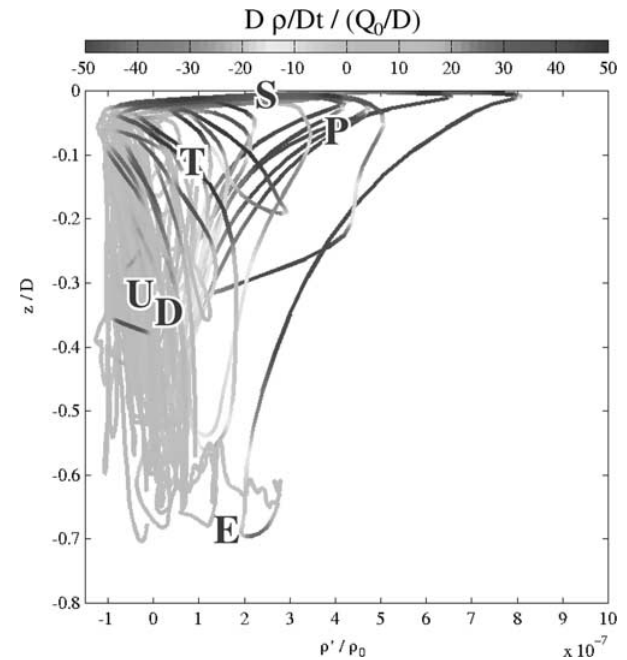
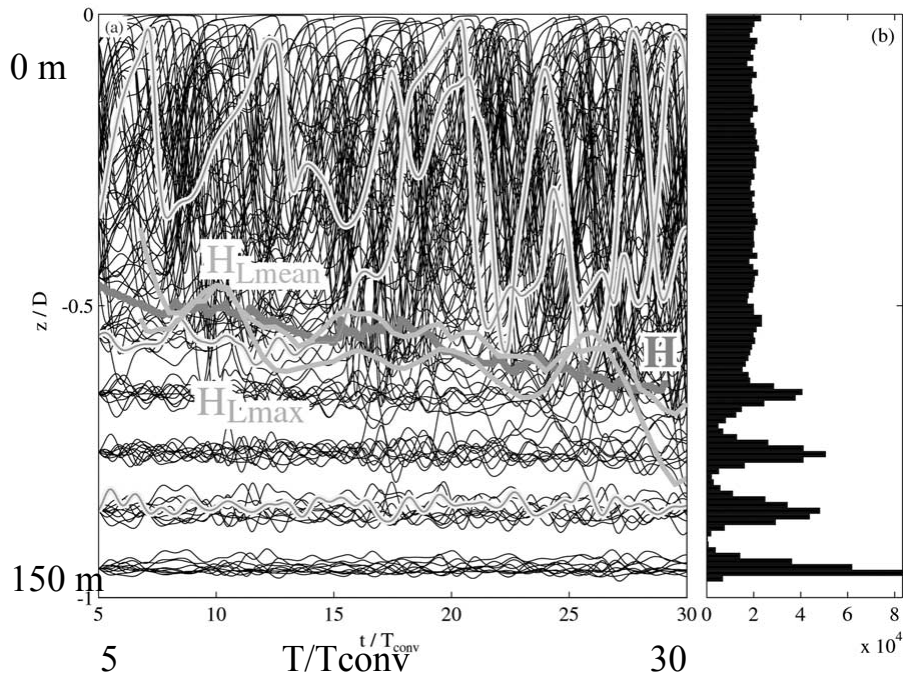


FIG. 16. Comparison of observed and fit rms vertical velocity. Rms vertical velocity (shaded) with 95% confidence limits with fit (solid) from the nonrotating scaling,  $(B_e H)^{1/3}$ , shown in line 3 of Table 3. Total buoyancy flux (dotted) and wind (dashed) are each scaled by best linear coefficients; small bars show scaling for meteorological variables.

**MODELS ?**

d'Asaro , Winters and Lien JGR May 2002  
 Lagrangian simulation in a 2D model (x, z, t)





**$T_{conv} = 50000s$**

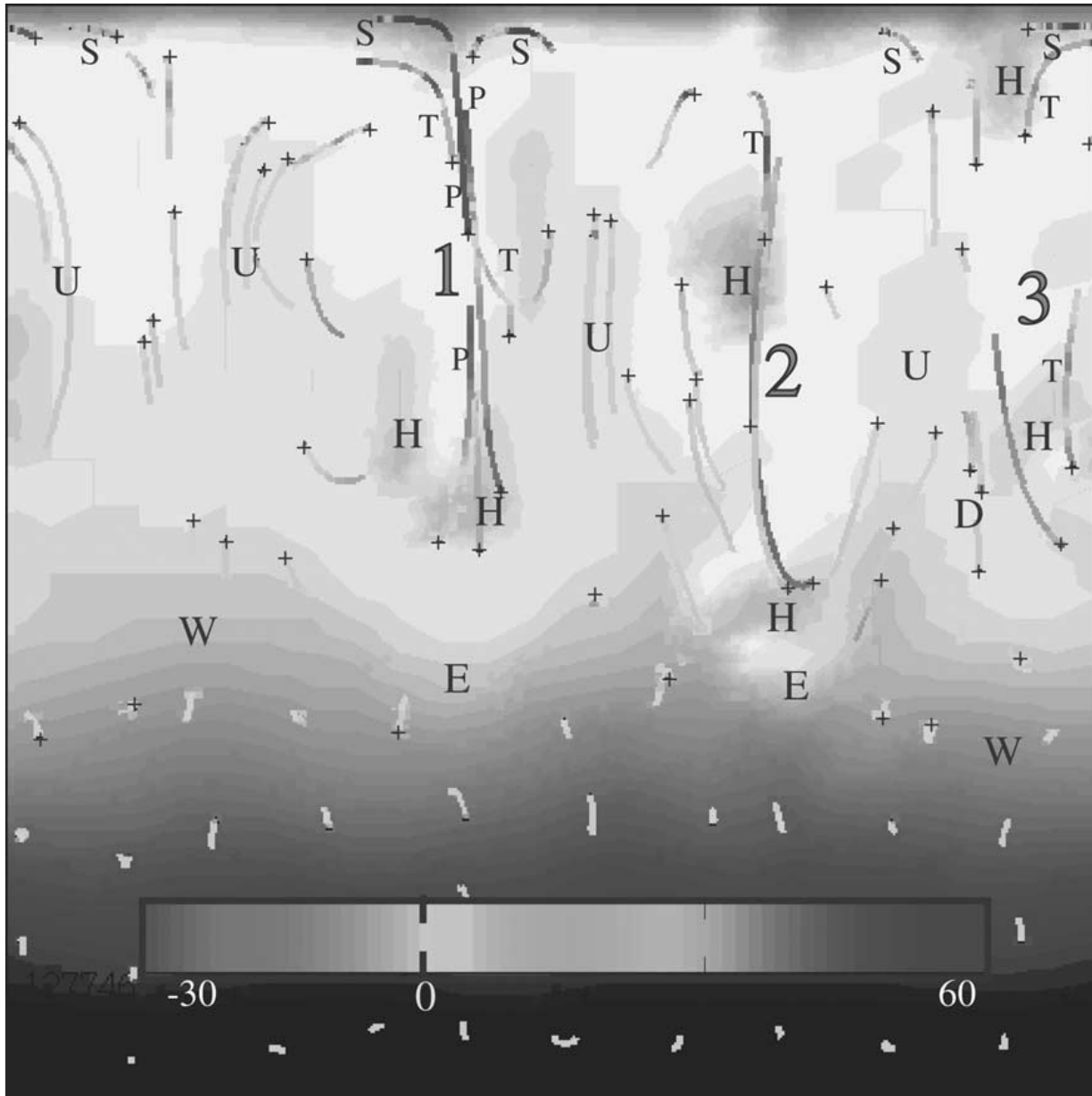
**S: Surface cooling    P: warming Plume**

**T cooling water Plume**

**U and D upwelling and downwelling between plumes**

**E entrainment below plume**

**Inside the mixing layer : equal probability for a par cel to occupy any depth for  $t > 25 T_{conv}$ . But for  $t =$  a few  $T_{conv}$  ?**



**X-Z view at**

**tv=14 TConv**

**+ marks end of trajectories for  $\frac{1}{2} T_{conv}$  before tv**

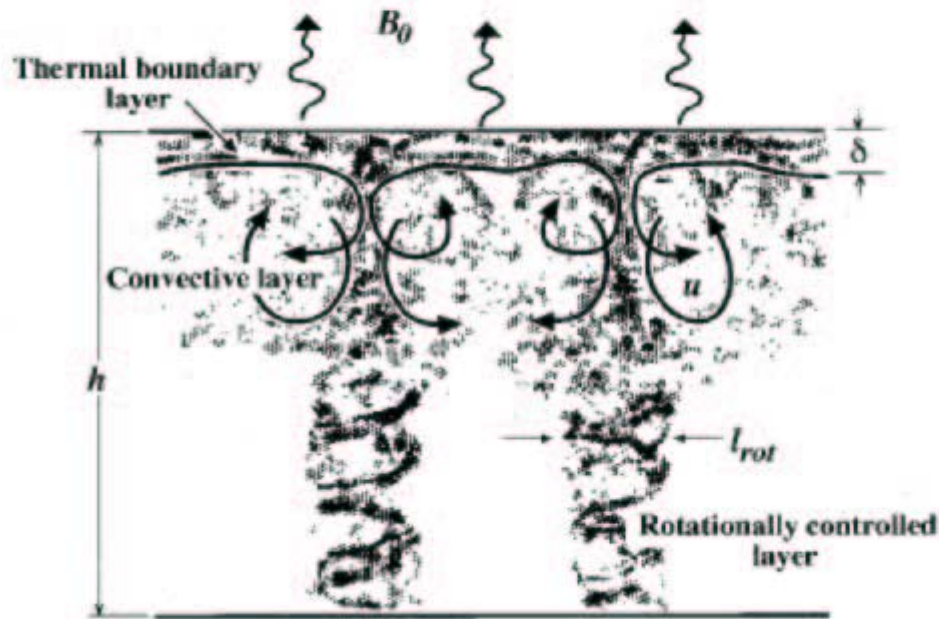


**Figure 19.** A schematic representation of the evolution of a population of plumes under rotational control sinking in to a homogeneous fluid of depth  $h$ , at a latitude where the Coriolis parameter is  $f$ , triggered by buoyancy loss  $\mathcal{B}_0$ . If the fluid is sufficiently deep (as drawn here) the plumes that make up the convective layer will come under rotational control on the scale  $l_{rot}$ .

then not possible to construct scales for the depth, however, as subsists of the plumes. The convective

$$b \sim b_{norot} = (\dots)$$

The subscript “norot” indicates adopted in the absence of rotation implicit in the flux law equation

### 3.3.1.2. Scale constrained

If  $h$  is sufficiently large then they come under geostrophic control at depth  $h$ . The transition from plumes to quasi-2-D, rotationally controlled (represented schematically in equation (11), the following scaling [Schott *et al.*, 1991]):

$$l \sim l_{rot} = (\dots)$$

$$u \sim u_{rot} = (\dots)$$

$$b \sim b_{rot} = (\dots)$$

where the subscript “rot” (for rotation) to denote the scales at which rotation is important. Golytsin [1980] attempted to write down the scales (13). For

processes in a similar way. The following scales can be formed from  $\mathcal{B}_0$  and  $t$  (a more detailed account is given by Jones and Marshall [1993] and Maxworthy and Narimousa [1994]):

$$l \sim (\mathcal{B}_0 t^3)^{1/2} \quad (11a)$$

$$u \sim w \sim (\mathcal{B}_0 t)^{1/2} \quad (11b)$$

$$b \sim (\mathcal{B}_0 t)^{1/2} \quad (11c)$$

where  $l$  is a measure of the scale of the convective elements.

**3.3.1.1. Scale constrained by the depth:** If it is the depth  $h$  that ultimately limits the scale of the cells then putting  $l = h$  in (11a), the following scaling is suggested [Deardorff, 1985], independent of rotation:

$$l \sim l_{\text{norot}} = h \quad (12a)$$

$$u \sim u_{\text{norot}} = (\mathcal{B}_0 h)^{1/3} \quad (12b)$$

At these scales the plume Rossby number is unity:

$$Ro = \frac{u}{f l} \sim \frac{u_{\text{rot}}}{f l_{\text{rot}}} = 1$$

It should be noted that the foregoing scales are independent of assumptions concerning eddy viscosity and diffusivity, provided that they are sufficiently small; they are the velocity, space, and buoyancy scales that can be constructed from the “external” parameters  $\mathcal{B}_0$ ,  $f$ , and  $h$ . However, the constants of proportionality in (12) and (13) will be dependent on viscous/diffusive processes and can be determined experimentally from laboratory and numerical experiments (see section 3.5.1 and equation (18)).

Helfrich [1994] has vividly illustrated possible rotational constraints on convective plumes in the laboratory. Figure 20 shows a sequence of photographs from an experiment in which a salt solution, dyed for flow

**TABLE 3. Velocity, Buoyancy, and Space Scaling in the Open-Ocean Deep Convection Regime**

Scaling	Heat Flux = 100 W m <sup>-2</sup> ; Buoyancy Flux = 5.00 × 10 <sup>-9</sup> m <sup>2</sup> s <sup>-3</sup>	Heat Flux = 500 W m <sup>-2</sup> ; Buoyancy Flux = 2.25 × 10 <sup>-7</sup> m <sup>2</sup> s <sup>-3</sup>	Heat Flux = 1000 W m <sup>-2</sup> ; Buoyancy Flux = 5.00 × 10 <sup>-7</sup> m <sup>2</sup> s <sup>-3</sup>	Heat Flux = 1500 W m <sup>-2</sup> ; Buoyancy Flux = 7.25 × 10 <sup>-7</sup> m <sup>2</sup> s <sup>-3</sup>	
$l_{\text{rot}}$ , km	$(\mathcal{B}_0/f^3)^{1/2}$	0.22	0.47	0.71	0.85
$u_{\text{rot}}$ , m s <sup>-1</sup>	$(\mathcal{B}_0/f)^{1/2}$	0.02	0.05	0.07	0.09
$u_{\text{norot}}$ , m s <sup>-1</sup>	$(\mathcal{B}_0 h)^{1/3}$	0.04	0.08	0.09	0.12
$Ro^*$	$\mathcal{B}_0^{1/2}/f^{3/2} h$	0.11	0.24	0.35	0.43
$l_p$ , km	$h \sqrt{Ro^*}$	0.67	0.97	1.19	1.31

Here  $h = 2$  km and  $f = 10^{-4}$  s<sup>-1</sup>.

From the surface to the bottom of the mixed layer under strong forcing , we succesively have

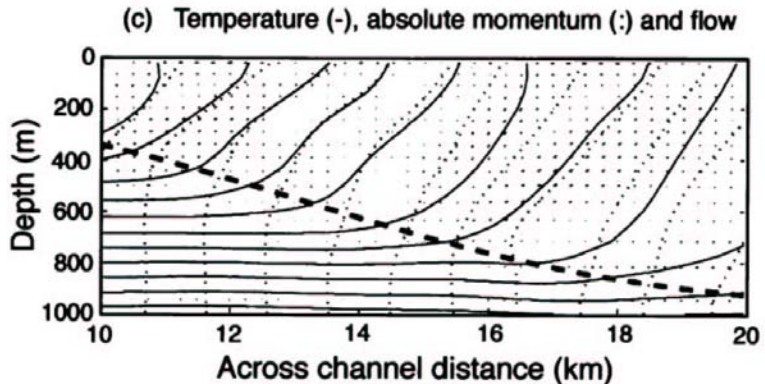
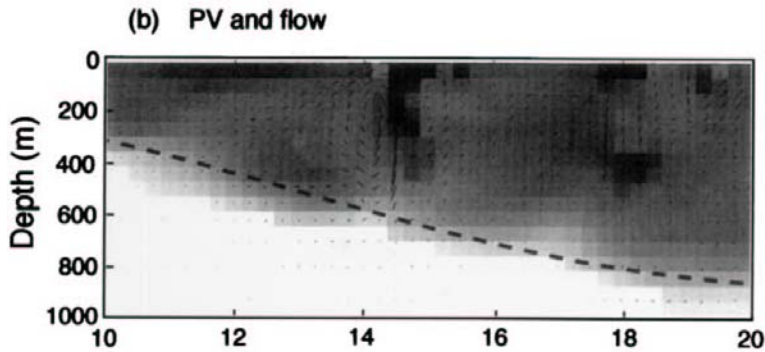
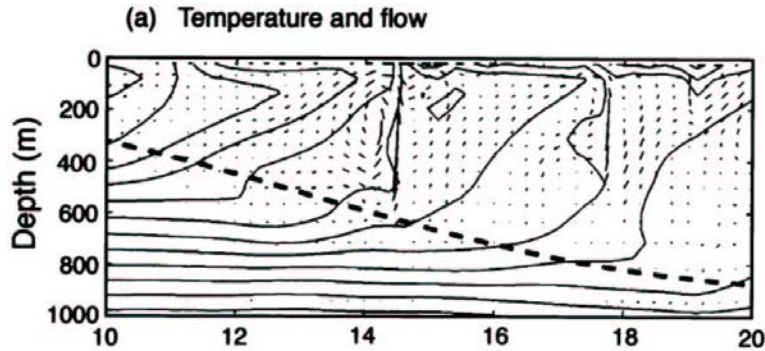
- thin (?) Surface Boundary Layer  
(few meters to 50 meters) strongly variable in time and depth
- Uprigth convection
- Rotational convection
- Remant layer

Was all ?

Haine and Marshall JPO 1997, 3d model constant buoyancy forcing,  
take into account the horizontal gradient of density (weak but sufficient to hor;gradient of U)

- Gravitational instability (« upright » convection)
- Symmetric instabilty convection with non zero vertical gradient but zero potential vorticity
- further: barocilic instability; time sacle of these processes are given.

Result in intermittence of turbulence and trajectories of parcel water!



Yaxis across the channel

## Case of symmetric instability

Trajectories are slanting along isopycnals

Residual (weak) stratification appears

Time of occurrence of this instability?

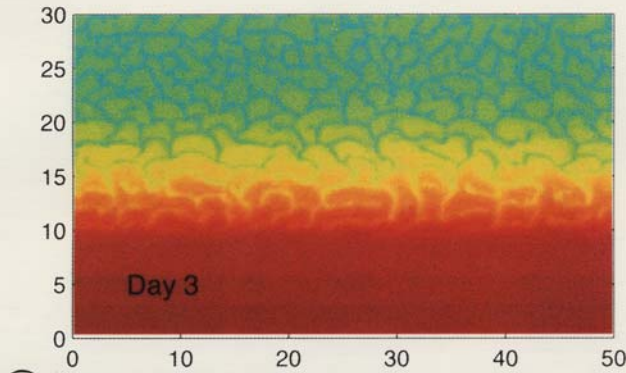
Dependent of  $(\zeta/f - 1/Ri)f^2 < 0$   $10/T^2$

$$\zeta = f - \delta u / \delta y$$

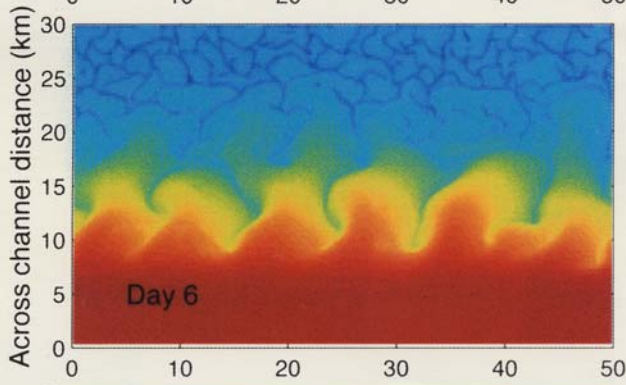
Ri Richardson number  $N^2 f^2 / M^4$

$$N^2 = -g / \rho \cdot \delta \rho / \delta z ; M^2 = | -g / \rho \cdot \delta \rho / \delta y |$$

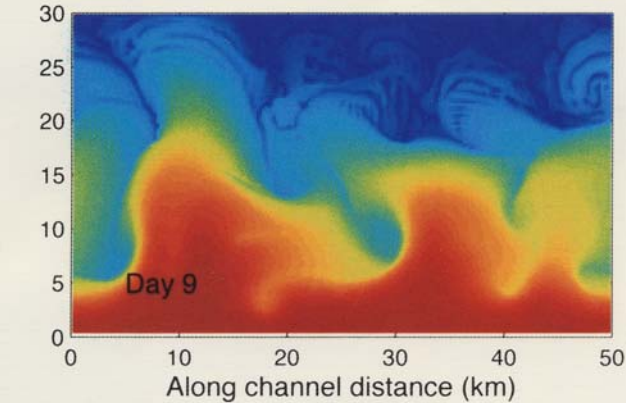
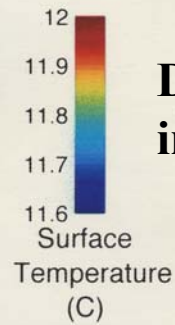
**After  
instability**



**Day 3  
upright  
convection**



**Day 6 symmetric  
instability ?**



**Day 9 baroclinic  
instability**

**Cycling time in mixing layer (depth is strongly variable in time) more than 1 cycle per day whatever the mixing layer depth**

**In the mixing layer each cell of phytoplankton receives the same irradiation for 2, 3, 4 days ( Is an relevant hypothesis ?)**

**What are the influence of the intermittence of lighth on growth cell?**

**We observed in February 1997 inside a 200km diameter anticyclonic eddy at 49°N 45 ° W (Caniaux, et al, GRL 2001) homogeneus concentration of phytoplankton down to 750 m !!!**

**$Q_e -700 \text{ w.m}^{-2}$  for 15 days ; SST 13 °C**

**Integrated biomass was circa 45 mg.m<sup>-2</sup> Chla , in Winter with low Chla concentration**

**Production inside thick mixed layer could be significative . Why?**

## References

Haine and Marshall 1998, *Journal of Physical Oceanography* , 28, 634-658

Denman and Gargett ,1983 , *Limnology and Oceanography*, 28 (5) 801-815

Marshall and Schott, 1999, *Reviews of Geophysics*, 37 (1) 1-65

Steffen and d'Asaro, 2002, *Journal of Physical Oceanography* , 32 (2) 475- 492

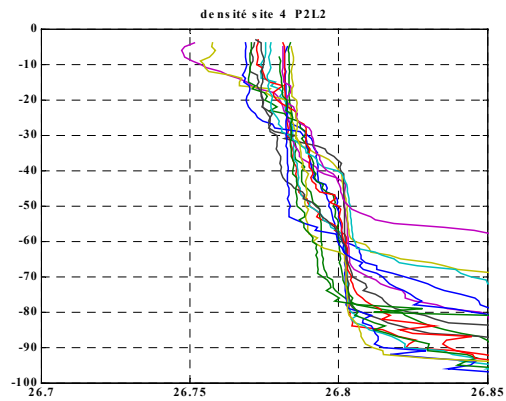
All articles in *JPO* 32(2) 2002 an issue on Deep Convection

Brainerd and Gregg, 1995, *Deep Sea Research*, 42 (9), 1521-1543

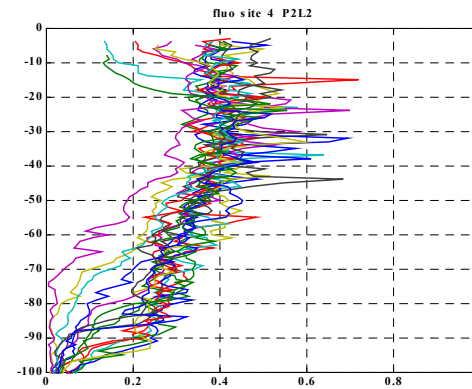
Thorpe , 1995, *Progress in Oceanography*, 35 315 –352, a review of dynamical processes of transfer at the sea surface

# Site 4 Pomme 2 Leg 2

## rau



## Fluo



## S

